DEUTSCHES ELEKTRONEN-SYNCHROTRON DESY

DESY 88-007
January 1988

THE WIDTH OF THE Z BOSON

by

W. Beenakker

Instituut Lorentz, Leiden University, The Netherlands

W. Hollik

II. Institut für Theoretische Physik, Universität Hamburg
F.R. Germany

ISSN 0418-9833

NOTKESTRASSE 85 · 2 HAMBURG 52

DESY 88-007
January 1988

ISSN 0418-9833

The Width of the Z Boson

WIM BEENAKKER *
INSTITUUT LORENTZ
LEIDEN UNIVERSITY, THE NETHERLANDS
AND
WOLFGANG HOLLIK
II. INSTITUT FÜR THEORETISCHE PHYSIK
UNIVERSITÄT HAMBURG, FRG

Abstract

We present a detailed discussion of the electroweak radiative corrections to the partial decay widths of the Z boson into lepton and quark pairs ($q \neq t$) and to the total width for 5 flavors. The results are only very weakly dependent on the Higgs mass. The top mass dependence leads to sizable variations of Γ_Z which have to be taken into account for precision experiments at the e^+e^- colliders LEP and SLC.

*supported by the Stichting FOM

1 Introduction.

One of the basic measurements at the near future e^+e^- colliders LEP and SLC will be the determination of the shape of the Z resonance. This will provide us with two of the most interesting and important electroweak parameters: the mass and the width of the neutral vector boson. For precision tests of the Standard Model and for searches for signals of possible new physics it is indispensible to know the predictions of the Standard Model with high accuracy, including higher order corrections. The QED corrections /1/, in particular real and virtual photonic corrections in the initial state, constitute the largest part of the radiative corrections and lead to a distortion of the shape of the resonance and to a shift in the peak value. In view of the high accuracy with which the mass and width will probably be measured ($\pm$20 MeV /2/) we are forced to go beyond the O(α) contributions in these observables. The effect of O(α^2) initial state radiation on the Z shape has been studied in /3/. It was found that the 2-loop QED corrections cause a shift in the Z peak value by +84 MeV. Combined effects of initial state bremsstrahlung and weak corrections in the Z propagator, i.e. the s-dependence of the width and 2-loop corrections to the imaginary part of the Z self energy, have also been investigated recently /4/.

The higher order corrections to the Z width are therefore of twofold importance:

- They influence the shape of the resonance and have consequently to be considered for precision measurements of the Z mass.
- The partial widths for $Z \to f\bar{f}$ will allow one to study the weak coupling constants of the various fermions at the level of quantum corrections.

In this note we discuss in detail the radiative corrections to $\Gamma(Z \to f\bar{f})$, $f = \nu,\ l,\ q(\neq t)$, which enter the results presented in /4/. Previous calculations have been performed for the leptonic widths /5/ and also for $Z \to q\bar{q}$ /6,7/. In /7/ the influence of the top quark on the $Z \to b\bar{b}$ decay width has been considered in a unitary gauge calculation.

The underlying schemes for the various calculations, however, as well as the choice of the input parameters, are different in general, and a numerical comparison at the high precision level as required nowadays has not been performed so far. Moreover, the on-shell renormalization scheme based on the boson masses M_W, M_Z together with the electromagnetic fine structure constant $\alpha = 1/137.03604$ has become generally accepted meanwhile and has been widely used also in other practical applications (ref's 8-10 and references therein).

The basis for our calculation is the on-shell scheme as specified in /12/. In contrast to /7/ we perform our calculation in the renormalizable t'Hooft-Feynman gauge. Since we have to include virtual top quarks and unphysical Higgs bosons in the $Z \to q\bar{q}$ decay vertex corrections the renormalization procedure of /12/ has to be extended keeping finite mass effects of the type m_t^2/M_W^2.

QCD corrections in $Z \to q\bar{q}$ decays are not explicitly discussed. They can easily be included by multiplying the electroweak partial widths $\Gamma_{ew}(f\bar{f})$ by the QCD correction factor /22/ yielding ($f \neq t$)

$$\Gamma_{ew+QCD}(f\bar{f}) = \Gamma_{ew}(f\bar{f})\left(1 + \frac{3}{8}\frac{\alpha_s(M_Z^2)}{\pi}\frac{(N_C^f)^2-1}{N_C^f}\right) \quad (1.1)$$

with the color factor

$$N_C^f = 3 \quad (\text{quarks}), \qquad N_C^f = 1 \quad (\text{leptons}). \quad (1.2)$$

Electroweak corrections to open top final states in case of $m_t < M_Z/2$, a possibility which is experimentally not completely ruled out, have been considered in /13/. They are less important in view of the uncertainties from the top mass in the phase space factors and from large QCD corrections near threshold /17/. Therefore in this article we study the case $m_t > M_Z/2$.

The paper is organized as follows: Section 2 contains the tree level results and the specification of our notation; in Section 3 we include the electroweak corrections to the partial widths, and Section 4 gives numerical results and a comparison with previous work. Relevant formulae including the top dependent vertex corrections are put together in the Appendix.

2 Notations and tree level results

In lowest order the Z propagator has the Breit-Wigner form

$$D_Z^0(s) = \frac{1}{s - M_Z^2 + iM_Z\Gamma_Z^0}. \quad (2.1)$$

The lowest order total width Γ_Z^0 is related to the one-loop self energy $\Sigma_Z(s)$ of the Z boson by

$$M_Z\Gamma_Z^0 = Im\ \Sigma_Z(s = M_Z^2). \quad (2.2)$$

It can be written as the sum of the partial fermionic decay widths $\Gamma_Z^0(f\bar{f})$ with $m_f < M_Z/2$:

$$\Gamma_Z^0(f\bar{f}) = \sum_f \Gamma_Z^0(f\bar{f}). \quad (2.3)$$

These partial widths can be expressed in terms of the vector and axialvector coupling constants of the fermion f to the Z

$$v_f = \frac{I_f^3 - 2Q_f s_W^2}{2s_W c_W} \quad (2.4)$$

$$a_f = \frac{I_f^3}{2s_W c_W}$$

with

$$s_W = \sin\theta_W, \quad c_W = \cos\theta_W$$

as follows:

$$\Gamma_Z^0(f\bar{f}) = N_C^f\,\frac{\alpha}{3}\,M_Z\,\sqrt{1-4\mu_f}\,\left(v_f^2(1+2\mu_f) + a_f^2(1-4\mu_f)\right) \quad (2.5)$$

with

$$\mu_f = \frac{m_f^2}{M_Z^2} \quad (2.6)$$

and the color factor N_C^f, eq. (1.2). The mixing angle is used in the standard on-shell definition in terms of the boson masses:

$$s_W^2 = 1 - \frac{M_W^2}{M_Z^2}. \quad (2.7)$$

For actual calculations the dependence on M_W is eliminated in favor of the precisely measured Fermi constant G_μ by means of the relation /14/

$$M_W^2(1 - M_W^2/M_Z^2) = \frac{A}{1 - \Delta r(\alpha, M_W, M_Z, M_H, m_t)} \quad (2.8)$$

with

$$A = \frac{\pi\alpha}{\sqrt{2}G_\mu} = (37.281GeV)^2.$$

For our calculation we use the expression Δr in the form as given in /11,12/.

3 Electroweak one-loop contributions

The partial widths (2.5) in lowest order are influenced by next order corrections in terms of the vector boson 2-point functions, external wave function renormalization of the fermions, and irreducible vertex corrections. In the following all symbols for the loop contributions denote the corresponding renormalized finite quantities. The explicit expresssions for the 2-point functions can be found in /12/.

The Z propagator (2.1) becomes modified replacing the constant width term by the Z boson self energy $\Sigma_Z(s)$:

$$D_Z(s) = \frac{1}{s - M_Z^2 + Re\Sigma_Z(s) + i\,Im\Sigma_Z(s)} \quad (3.1)$$

where Re $\Sigma_Z(M_Z^2) = 0$ due to the on-shell renormalization condition for the Z boson. Around the Z pole approximately a Breit-Wigner form

$$D_Z(s) = \frac{1}{1 - \Pi_Z(M_Z^2)}\,\frac{1}{s - M_Z^2 + iM_Z\Gamma_Z^{(1)}} \quad (3.2)$$

is recovered by a re-definition of the total width

$$\Gamma_Z^{(1)} = \frac{\Gamma_Z^0}{1 - \Pi_Z(M_Z^2)} \quad (3.3)$$

with Γ_Z^0 from (2.3-5) and

$$\Pi_Z(s) = -\frac{\partial}{\partial s}\,Re\ \Sigma_Z(s). \quad (3.4)$$

This global normalization (3.3) corresponds to the wave function renormalization of the Z line in the decay diagram 1a. For each partial width this means that (2.5) has to be multiplied by a common factor:

$$\Gamma_Z^{(1)}(f\bar{f}) = \Gamma_Z^0(f\bar{f})\cdot\left(1 - \Pi_Z(M_Z^2)\right)^{-1}. \qquad (3.5)$$

Furthermore, the relation (2.8) can be utilized in order to re-express (2.5) in terms of the Fermi constant G_μ, yielding:

$$\Gamma_Z^{(1)}(f\bar{f}) = \bar{\Gamma}_Z^0(f\bar{f})\,\frac{1-\Delta r}{1-\Pi_Z(M_Z^2)}. \qquad (3.6)$$

The quantity

$$\bar{\Gamma}_Z^0(f\bar{f}) = N_C^f\,\frac{G_\mu M_Z^3}{24\pi\sqrt{2}}\,\sqrt{1-4\mu_f}\,\left(1-4\mu_f+(2I_f^3-4Q_f s_W^2)^2\,(1+2\mu_f)\right) \qquad (3.7)$$

represents another possible tree level parametrization of the partial decay width leading to an approximate total width [1]

$$\bar{\Gamma}_Z^0 = \sum_f \bar{\Gamma}_Z^0(f\bar{f}). \qquad (3.7a)$$

Since the large contributions from the light fermions

$$\frac{\alpha}{3\pi}\sum_f Q_f^2\,\log\frac{M_W^2}{m_f^2}$$

in Δr and in $\Pi_Z(M_Z^2)$ cancel in the expression (3.6), $\bar{\Gamma}_Z^0$ turns out to be a sufficiently good approximation (for $m_t < 100$ GeV) including already the major part of the one-loop corrections.

In addition to (3.6) we have to incorporate the γ-Z mixing contribution (Figure 1b) and the vertex corrections together with the external fermion self energies (Figures 2,3). Since we do not consider radiative corrections to $Z \to t\bar{t}$ we can neglect all terms of order m_f^2/M_Z^2 $(f \neq t)$ in the loop expressions. This means that also Higgs contributions in vertex and fermion self energy diagrams are neglected, except for $f = b$.

In case of the $Z \to b\bar{b}$ decay channel the full top mass dependence coming from the virtual t quarks in Figures 2,3 is included. Due to the underlying 't Hooft-Feynman gauge also "unphysical" charged Higgs bosons enter the diagrams as virtual states with poles at $q^2 = M_W^2$.

The final result for the partial width can be written in the following way:

$$\Gamma_Z(f\bar{f}) = \left(\Gamma_Z^0(f\bar{f}) + \Delta\Gamma_Z(f\bar{f})\right)\cdot\left(1-\Pi_Z(M_Z^2)\right)^{-1} \qquad (3.8)$$

with $\Gamma_Z^0(f\bar{f})$ from (2.5), and

[1] Others than $Z \to f\bar{f}$ decay channels in higher order of the coupling constant are very small /21/ and can be neclected for our discussion of the total width

$$\Delta\Gamma_Z(f\bar{f}) = N_C^f\,\frac{2}{3}\,\alpha M_Z\,\left(v_f\,(F_V^f + Q_f\Pi_{\gamma Z}) + a_f F_A^f\right). \qquad (3.9)$$

The γ-Z mixing term is related to the mixing energy $\Sigma_{\gamma Z}$:

$$\Pi_{\gamma Z} = Re\,\Sigma_{\gamma Z}(M_Z^2)/M_Z^2. \qquad (3.10)$$

$\Sigma_{\gamma Z}$ is taken from /12/. The finite vector and axialvector form factors $F_{V,A}^f$ are listed in the appendix for the various types of fermions.

Finally we have to include the QED corrections due to virtual photon exchange and real bremsstrahlung integrated over the full phase space. For light final fermions the result can be simply obtained /21/ by multiplying (3.8) with the correction factor $1+\delta_{QED}^f$, with

$$\delta_{QED}^f = \frac{3\alpha}{4\pi}\,Q_f^2. \qquad (3.11)$$

Its relative influence is $< 0.17\%$.

4 Results and discussion

Besides the quantities α, $G\mu$, M_Z, which are sufficient to determine Γ_Z at the tree level, the unknown parameters M_H and m_t enter the higher order result. For our numerical discussion we proceed in the following way:

After specifying the values for M_Z, M_H, m_t we derive from (2.8) the corresponding value for M_W resp. $\sin^2\theta_W$ thus fixing the coupling constants v_f, a_f and the next order terms in (3.8-9). To this end we have to specify the hadronic vacuum polarization from the light quarks which enters the quantity Δr in (2.8) as well as the Z wave function renormalization $\Pi_Z(M_Z^2)$. We do this by adjusting our hadronic QED part of Δr to the result of Jegerlehner /15/, which, for 5 flavors, is ($M_Z = 93$ GeV):

$$\Delta r_{had,QED}^{(5)} = 0.0286 \pm 0.0007. \qquad (4.1)$$

This is slightly different from the by 0.0012 lower value in /16/ adopted in /7/. In order to perform a comparison with /7/ we have to modify our hadronic input accordingly.

Table 1 contains the total electroweak Z width Γ_Z (including QED corrections) for fixed $M_H = 100$ GeV. The tree level values Γ_Z^0 correspond to the standard parametrization given in (2.3-5), $\bar{\Gamma}_Z^0$ is the tree level width (3.7a) in the G_μ representation. For top masses not too large ($m_t < 100$ GeV) $\bar{\Gamma}_Z^0$ gives already an approximation which is good within 5 MeV. For large top masses, however, $\bar{\Gamma}_Z^0$ becomes insufficient as well; in some cases the parametrization Γ_Z^0 in (2.5) is the better approximation.

The Higgs and top mass dependences of the total width Γ_Z are put together in Table 2 for various Z masses. The variation with m_t is strong enough that it has to be respected in view of a 10 MeV precision. For example, the variation of m_t between 50 and 150 MeV leads to an inrease in Γ_Z by 21 MeV (for $M_Z = 92$ GeV, $M_H = 100$ GeV). On the other hand, the variation of Γ_Z with the Higgs mass remains smaller than 10 MeV.

The hadronic uncertainty coming from (4.1) is responsible for a hadronic uncertainty in Γ_Z amounting to $(\Delta\Gamma_Z)_{had} = \pm 0.6$ MeV. The somewhat larger hadronic error in the photon vacuum polarization of ± 0.0012, as estimated in /19/, results in $(\Delta\Gamma_Z)_{had} = \pm 1$ MeV. In both cases the uncertainty coming from the light quarks is of no practical importance for Γ_Z.

Next we discuss the partial decay widths for $Z \to f\bar{f}$ and their dependence on the model parameters, listed in Table 3. Again, the variation with the Higgs mass is not very striking: 0.2 MeV for the leptonic channels, and somewhat more in the hadronic decay modes, but still smaller than 1 MeV.

The dependence on m_t is strongest in the $Z \to u\bar{u}$ and $Z \to d\bar{d}$ decays. In the $Z \to b\bar{b}$ partial width, however, the top mass dependence is much weaker. The reason for this behaviour is the additional top dependence of the vertex corrections in $Z \to b\bar{b}$ which cancels (partly) the top contributions in the gauge boson 2-point functions. This is exhibited in more detail in Table 4 (for $M_Z = 92$ GeV, $M_H = 100$ GeV):

The tree level approximations $\bar{\Gamma}^0_Z(f\bar{f})$ as defined in (3.7) are slightly different for d and b quarks due to the finite m_b. The determination of $\sin^2\theta_W$ by means of (2.8) and the dependence of Δr on m_t are responsible for the variation of $\bar{\Gamma}^0_Z(f\bar{f})$ with the value of m_t. The weak corrections $\Delta\Gamma^{weak}_Z(f\bar{f})$ defined as

$$\Delta\Gamma^{weak}_Z(f\bar{f}) = \Gamma_Z(f\bar{f}) - \bar{\Gamma}^0_Z(f\bar{f}) \quad (4.2)$$

with the corrected partial width $\Gamma_Z(f\bar{f})$ from (3.8) induce additional top quark contributions. Those entering via the Z-Z and Z-γ propagators (Figure 1) are identical for both d and b, whereas the vertex and quark self energy diagrams (Figures 2,3) yield different corrections for d and b final states. For $b\bar{b}$ they tend to cancel the increase of the lowest order term for larger m_t.

Finally we want to compare our results with those of the previous calculations by Wetzel /6/ and Akhundov et al /7/. Wetzel employs a different renormalization scheme ; therefore only a comparison of the corrected values for $\Gamma_Z(f\bar{f})$ is meaningful. For $M_Z = 92$ GeV, $M_H = 100$ GeV and $m_t = 40$ GeV, as specified in /6/, we find agreement within 0.5 MeV for the ν, e, u, and d partial widths. Heavy quarks are not discussed in detail in /6/.

In order to make our results comparable with those of Akhundov et al /7,20/, obtained in the on-shell scheme and the unitary gauge, we have to put $m_b = 0$ in the tree level formula and to adjust our value for hadronic QED vacuum polarization in a way that it fits the table for $\sin^2\theta_W$ given by Lynn and Stuart /16/ (since their hadronic part was adopted in /7/).

Doing this, we find excellent agreement in all partial widths within 0.1 MeV, sometimes 0.2 MeV, for the whole range of the considered top and Higgs masses. This underlines the high level of reliability in the calculation of electroweak radiative corrections.

In conclusion, our discussion of the Z width has shown that the electroweak corrections play a role for precision experiments, in particular the top mass dependence. The variation with the Higgs mass does not exceed the aimed experimental accuracy.

5 Appendix

5.1 $Z \to f\bar{f}$ vertex corrections for $f \neq b$

For those external fermions which do not get virtual top contributions in the vertex diagrams only diagrams 2 a-c and 3 a,b have to be respected. The finite result after renormalization can be summarized in terms of vector and axialvector form factors:

$$\Gamma^{Zff}_\mu = ie\gamma_\mu\,(v_f - a_f\gamma_5) + ie\gamma_\mu\,\left(F^f_V(s) - \gamma_5\,F^f_A(s)\right). \quad (5.1)$$

The quantities $F^f_{V,A}$ entering the Z width formula in (3.9) are given by the on-resonance values

$$F^f_V = Re\,F^f_V(M_Z^2), \quad F^f_A = Re\,F^f_A(M_Z^2). \quad (5.2)$$

The explicit expressions for the form factors in (5.1) read for

Neutrinos :

$$F^\nu_V(s) = F^\nu_A(s) = \frac{\alpha}{4\pi}\,\frac{1}{4s_Wc_W}\left\{\frac{1}{4s_W^2c_W^2}\,\Lambda_2(s,M_Z) + \frac{2s_W^2-1}{2s_W^2}\,\Lambda_2(s,M_W) + \frac{3c_W^2}{s_W^2}\,\Lambda_3(s,M_W)\right\}$$

Charged leptons:

$$F^l_V(s) = \frac{\alpha}{4\pi}\left\{v_l(v_l^2+3a_l^2)\,\Lambda_2(s,M_Z) + F^l_L\right\} \quad (5.3)$$

$$F^l_A(s) = \frac{\alpha}{4\pi}\left\{a_l(3v_l^2+a_l^2)\,\Lambda_2(s,M_Z) + F^l_L\right\}$$

with

$$F^l_L = \frac{1}{8s_W^3c_W}\,\Lambda_2(s,M_W) - \frac{3c_W}{4s_W^3}\,\Lambda_3(s,M_W)$$

u-type quarks:

$$F^u_V(s) = \frac{\alpha}{4\pi}\left\{v_u(v_u^2+3a_u^2)\,\Lambda_2(s,M_Z^2) + F^u_L\right\}$$

$$F^u_A(s) = \frac{\alpha}{4\pi}\left\{a_u(3v_u^2+a_u^2)\,\Lambda_2(s,M_Z^2) + F^u_L\right\}$$

with

$$F^u_L = -\frac{1-\frac{2}{3}s_W^2}{8s_W^3c_W}\,\Lambda_2(s,M_W) + \frac{3c_W}{4s_W^3}\,\Lambda_3(s,M_W)$$

d-type quarks:

$$F^d_V(s) = \frac{\alpha}{4\pi}\left\{v_d(v_d^2+3a_d^2)\,\Lambda_2(s,M_Z^2) + F^d_L\right\}$$

$$F^d_A(s) = \frac{\alpha}{4\pi}\left\{a_d(3v_d^2+a_d^2)\,\Lambda_2(s,M_Z^2) + F^d_L\right\}$$

with

$$F^d_L = \frac{1-\frac{4}{3}s_W^2}{8s_W^3c_W}\,\Lambda_2(s,M_W) - \frac{3c_W}{4s_W^3}\,\Lambda_3(s,M_W)$$

In the range $m_f^2 << s < 4M_W^2$ the functions Λ_2, Λ_3 have the form [2] ($w = M^2/s$, where $M = M_Z$ or M_W)

$$\Lambda_2(s,M) = -\frac{7}{2} - 2w - (2w+3)\log(w) + 2(1+w)^2\left(\log(w)\log(\frac{1+w}{w}) - Li_2(-\frac{1}{w})\right),$$

$$\Lambda_3(s,M) = \frac{5}{6} - \frac{2w}{3} + \frac{2}{3}(2w+1)\sqrt{4w-1}\,\arctan\frac{1}{\sqrt{4w-1}}$$
$$-\frac{8}{3}w(w+2)\left(\arctan\frac{1}{\sqrt{4w-1}}\right)^2. \quad (5.4)$$

5.2 Vertex corrections for $Z \to b\bar{b}$

The situation for the $b\bar{b}$ final state is more complicated due to the presence of the top quark and the charged Goldstone Higgs bosons in virtual states.

The form factors according to (5.1) can be written in a way analogous to (5.3):

$$F_V^b(s) = \frac{\alpha}{4\pi}\left\{v_b(v_b^2 + 3a_b^2)\Lambda_2(s,M_Z) + F_L^b\right\}$$
$$F_A^b(s) = \frac{\alpha}{4\pi}\left\{a_b(3v_b^2 + a_b^2)\Lambda_2(s,M_Z) + F_L^b\right\} \quad (5.5)$$

F_L^b is the sum of the top dependent diagrams Figure 2 b-g and the Z-bb counter term /12/ involving the b quark self energy diagrams figure 3 b,c :

$$F_L^b = \sum_{i=b}^{g} Re\, F_i + \frac{\frac{2}{3}s_W^2 - 1}{4s_W c_W}\,\delta Z_L^{fin}. \quad (5.6)$$

δZ_L^{fin} is the finite part of the left-handed b-quark renormalization constant which would vanish for $m_t << M_W$:

$$\delta Z_L^{fin} = \frac{1}{2s_W^2}(2 + \frac{m_t^2}{M_W^2})\left(\bar{B}_1(m_b^2, m_t, M_W) + m_b^2\bar{B}_1'(m_b^2, m_t, M_W)\right)$$
$$\cong \frac{1}{2s_W^2}(2 + \frac{m_t^2}{M_W^2})\,\bar{B}_1(m_b^2, m_t, M_W). \quad (5.7)$$

For the function $\bar{B}_1$ see equation (5.14) .

The F_i in (5.6) are the expressions corresponding to the diagrams Figure 2 b-g after subtracting those (divergent) parts which are cancelled by the vertex counter term after renormalization:

[2] Since we need only the real parts we drop here the imaginary parts

$$F_b = \frac{v_t + a_t}{4s_W^2}\left\{-\frac{3}{2} + 2\log\frac{M_W}{m_t} + 4\,C_2^0(s, m_t, m_t, M_W)\right.$$
$$-2s\left(C_2^+(s, m_t, m_t, M_W) - C_2^-(s, m_t, m_t, M_W)\right)$$
$$\left.+4s\,C_1^+(s, m_t, m_t, M_W) - 2s\,C_0(s, m_t, m_t, M_W)\right\}$$
$$-\frac{v_t - a_t}{4s_W^2}\,2m_t^2\,C_0(s, m_t, m_t, M_W) \quad (5.8)$$

$$F_c = -\frac{c_W}{4s_W^3}\left\{-\frac{3}{2} + 12\,C_2^0(s, M_W, M_W, m_t)\right.$$
$$-2s\left(C_2^+(s, M_W, M_W, m_t) - C_2^-(s, M_W, M_W, m_t)\right)$$
$$\left.+4s\,C_1^+(s, M_W, M_W, m_t)\right\}$$

$$F_d = \frac{v_t - a_t}{4s_W^2}\left(\frac{m_t}{M_W}\right)^2\left\{-\frac{3}{4} + log\frac{M_W}{m_t} + 2\,C_2^0(s, m_t, m_t, M_W)\right.$$
$$\left.-2s\left(C_2^+(s, m_t, m_t, M_W) - C_2^-(s, m_t, m_t, M_W)\right)\right\}$$
$$-\frac{v_t + a_t}{4s_W^2}\left(\frac{m_t}{M_W}\right)^2 m_t^2\,C_0(s, m_t, m_t, M_W)$$

$$F_e = \frac{s_W^2 - c_W^2}{8s_W^3 c_W}\left(\frac{m_t}{M_W}\right)^2\left\{-\frac{1}{4} + 2\,C_2^0(s, M_W, M_W, m_t)\right\}$$

$$F_f = F_g = -\frac{m_t^2}{4s_W c_W}\,C_0(s, M_W, M_W, m_t)$$

The functions C_1^+, C_2^+, C_2^-, C_2^0 are specified in terms of the scalar 3-point integral C_0 and the finite parts of the 2-point integrals $\bar{B}_0$, $\bar{B}_1$ defined below in (5.13-14):

$$(4m_b^2 - s)\,C_1^+(s, M, M, M') = \log\frac{M'}{M} + \bar{B}_0(s, M, M) - \bar{B}_0(m_b^2, M, M')$$
$$+(M'^2 - M^2 + m_b^2)\,C_0(s, M, M, M') \quad (5.9)$$

$$C_2^0(s, M, M, M') = \frac{1}{4}\left(\bar{B}_0(s, M, M) + 1\right) + \frac{1}{2}(M^2 - M'^2 - m_b^2)\,C_1^+(s, M, M, M')$$
$$+\frac{1}{2}M'^2\,C_0(s, M, M, M')$$

$$(4m_b^2 - s)\, C_2^+(s,M,M,M') = \frac{1}{2}\,\bar{B}_0(s,M,M) + \frac{1}{2}\left(\bar{B}_1(m_b^2,M',M) - \frac{1}{4}\right)$$
$$+(M'^2 - M^2 + m_b^2)\, C_1^+(s,M,M,M') - C_2^0(s,M,M,M')$$

$$s\, C_2^-(s,M,M,M') = -\frac{1}{2}\left(\bar{B}_1(m_b^2,M',M) - \frac{1}{4}\right) - C_2^0(s,M,M,M')$$

The scalar vertex integral for equal external masses m_f

$$\frac{i}{16\pi^2}\, C_0(s,M,M,M') = \int \frac{d^4k}{(2\pi)^4}\, \frac{1}{(k^2 - M'^2)\,((k-p_f)^2 - M^2)\left((k+p_{\bar{f}})^2 - M^2\right)} \qquad (5.10)$$

corresponds to the diagram

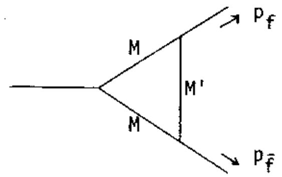

with

$$s = (p_f + p_{\bar{f}})^2, \quad p_f^2 = p_{\bar{f}}^2 = m_f^2.$$

Applying the method of 't Hooft and Veltman /18/ the integral (5.10)

$$C_0(s,M,M,M') = -\int_0^1 dy \int_0^y dx\, \left(ay^2 + bx^2 + cxy + dy + ex + f\right)^{-1}$$

with

$$a = m_f^2, \quad b = -c = s, \quad d = M^2 - M'^2 - m_f^2, \quad e = 0, \quad f = M'^2 - i\epsilon$$

is expressed in terms of dilogarithms[3]

$$C_0(s,M,M,M') = \frac{1}{c+2\alpha b} \sum_{l=1}^{3} \sum_{j=1}^{2} (-1)^l \left\{ Li_2\left(\frac{x_l}{x_l - y_{lj}}\right) - Li_2\left(\frac{x_l - 1}{x_l - y_{lj}}\right)\right\} \qquad (5.11)$$

together with

$$\alpha = \frac{1}{2}\left(1 - \sqrt{1 - \frac{4m_f^2}{s}}\right)$$

[3] Because we are dealing with real internal masses no extra logarithms from crossing some cuts have to be added

and

$$x_1 = -\frac{d + 2a + c\alpha}{c + 2\alpha b}, \qquad (5.12)$$
$$x_2 = -\frac{d}{(1-\alpha)(c+2\alpha b)},$$
$$x_3 = \frac{d}{\alpha(c + 2\alpha b)},$$

$$y_{1j} = \frac{-c \pm \sqrt{c^2 - 4b(a+d+f)}}{2b},$$
$$y_{2j} = y_{3j} = \frac{-d \pm \sqrt{d^2 - 4f(a+b+c)}}{2a}.$$

Finally we have to specify the functions $\bar{B}_0$ and $\bar{B}_1$ appearing in in (5.7) and (5.9).

$\bar{B}_0$ is the finite part of the scalar one-loop integral B_0 :

$$B_0(s,M,M') = \frac{1}{2}(\Delta_M + \Delta_{M'}) + \bar{B}_0(s,M,M')$$

with

$$\Delta_M = \frac{2}{4-D} - \gamma + \log\frac{4\pi\mu^2}{M^2},$$

and

$$\bar{B}_0(s,M,M') = 1 - \frac{M^2 + M'^2}{M^2 - M'^2}\log\frac{M}{M'} + F(s,M,M') \qquad (5.13)$$
$$= -\int_0^1 dx\, \log\frac{x^2 s - x(s + M^2 - M'^2) + M^2 - i\epsilon}{M\,M'}.$$

The analytic expression for the function $F(s,M,M')$ can be found in /12/.

The finite function $\bar{B}_1$ is related to F in the following way:

$$\bar{B}_1(s,M,M') = -\frac{1}{4} + \frac{M^2}{M^2 - M'^2}\log\frac{M}{M'} + \frac{M'^2 - M^2 - s}{2s}\,F(s,M,M'). \qquad (5.14)$$

It is the finite part of the 2-point integral

$$\frac{i}{16\pi^2}\, q_\mu\, B_1(q^2,M,M') = \mu^{4-D}\int \frac{d^Dk}{(2\pi)^D}\, \frac{k_\mu}{(k^2 - M^2)\,((q+k)^2 - M'^2)}$$

defined with the following subtraction:

$$B_1(s,M,M') = -\frac{1}{2}(\Delta_{M'} + \frac{1}{2}) + \bar{B}_1(s,M,M').$$

Acknowledgement

We are grateful to D.Yu.Bardin for supplying us with detailed information on the numerical results of the Dubna group. In particular we want to thank G.J.H. Burgers for numerous valuable discussions.

References

/1/ M.Greco, G. Pancheri, Y. Srivastava, Nucl. Phys. B 171 (1980) 118; E: B 197 (1982) 543
F.A. Berends, R. Kleiss, S. Jadach, Nucl. Phys. B 202 (1982) 63
M. Böhm, W. Hollik, Nucl. Phys. B 204 (1982) 45
/2/ Physics with LEP, ed. J.Ellis and R. Peccei, CERN 86-02
/3/ F.A. Berends, G.J.H. Burgers, W.L. van Neerven, Phys. Lett. 185 B (1987) 395; CERN-TH 4772/87
/4/ F.A. Berends, G.J.H. Burgers, W. Hollik, W.L. van Neerven, CERN-TH 4919/87
/5/ M.Consoli, S. LoPresti, L. Maiani, Nucl. Phys. B 223 (1983) 474;
P. Antonelli, M. Consoli, C. Corbo, Phys. Lett. 99 B (1981) 475;
F. Jegerlehner, Z. Phys. C 32 (1986) 425
/6/ W. Wetzel, in /2/, and Nucl. Phys. B 227 (1983) 1
/7/ A.A. Akhundov, D.Yu. Bardin, T. Riemann, Nucl. Phys. B 276 (1986) 1
/8/ Radiative Corrections in SU(2)×U(1), ed. B.W. Lynn and J. Wheater, Singapore 1984
/9/ A. Barroso et al, CERN-EP/87-70, in:
ECFA Workshop on LEP 200, ed. A.Böhm, W. Hoogland, CERN 87-08, ECFA 87-108
/10/ W. Hollik, EPS Conference on High Energy Physics, Uppsala 1987, and DESY Preprint DESY 87-129
/11/ M. Böhm, W. Hollik, H. Spiesberger, Z. Phys. C 27 (1985) 523
/12/ M. Böhm, W. Hollik, H. Spiesberger, Fortsch. Phys. 34 (1987) 687
/13/ W. Beenakker, W. Hollik, in /9/
/14/ A. Sirlin, Phys. Rev. D 22 (1980) 971
/15/ F. Jegerlehner, Z. Phys. C 32 (1986) 195
/16/ B.W. Lynn, R.G. Stuart, Nucl. Phys. B 253 (1985) 216
/17/ J. Jersak, E. Laerman, P.M. Zerwas, Phys. Rev. D 25 (1980) 1218
/18/ G. 't Hooft, M. Veltman, Nucl. Phys. B 135 (1979) 365
/19/ J. Cole, G. Penso, C. Verzegnassi, Trieste Preprint 19/85/EP (1985)
/20/ D.Yu. Bardin, private communication
/21/ W.J. Marciano, D. Wyler, Z. Phys. C 3 (1979) 81;
D. Albert, W.J. Marciano, D. Wyler, Nucl. Phys. B 166 (1980) 460
/22/ T.H. Chang, K.J.F. Gaemers, W.L. van Neerven, Nucl. Phys. B 202 (1982) 407

Table captions

Table 1 :
Total Z width without QCD corrections. All values in GeV.
Γ_Z^0 : tree level width, parametrization (2.3-5),
$\tilde{\Gamma}_Z^0$: tree level width, parametrization (3.7),
Γ_Z : with electroweak corrections.

Table 2 :
Total Z width including electroweak corrections (no QCD corrections).
All values in GeV.

Table 3 a :
Partial leptonic widths without QED corrections.
All values in GeV.

Table 3 b :
Partial hadronic decay widths without QED and QCD corrections.
All values in GeV.

Table 4 :
Partial widths for $Z \to d\bar{d}$ and $Z \to b\bar{b}$ in GeV.
$\tilde{\Gamma}_Z^0$: tree level approximation, eq. (3.7)
$\Delta\Gamma_Z^{weak}$: weak corrections, eq. (4.2)
$m_b = 4.5$ GeV, $M_Z = 92$ GeV, $M_H = 100$ GeV.

Figure captions

Figure 1:
Contributions of the vector boson 2-point functions to the $Z \to f\bar{f}$ width.

Figure 2:
Weak vertex corrections to the $Z \to f\bar{f}$ width.
f' denotes the isospin partner of the fermion f.

Figure 3:
Weak contributions to the fermion self energy.

Table 1

M_Z	m_t	Γ_Z^0	$\hat{\Gamma}_Z^0$	Γ_Z
90.	50.	2.1305	2.2936	2.2948
90.	100.	2.1739	2.3056	2.3035
90.	200.	2.2966	2.3386	2.3275
91.	50.	2.2176	2.3889	2.3898
91.	100.	2.2648	2.4019	2.3993
91.	200.	2.3997	2.4379	2.4244
92.	50.	2.3071	2.4869	2.4876
92.	100.	2.3584	2.5010	2.4978
92.	200.	2.5062	2.5401	2.5240
93.	50.	2.3992	2.5878	2.5881
93.	100.	2.4545	2.6029	2.5992
93.	200.	2.6161	2.6451	2.6264
94.	50.	2.4938	2.6914	2.6911
94.	100.	2.5531	2.7075	2.7033
94.	200.	2.7295	2.7531	2.7316
95.	50.	2.5910	2.7978	2.7968
95.	100.	2.6543	2.8149	2.8102
95.	200.	2.8464	2.8639	2.8396
96.	50.	2.6907	2.9070	2.9049
96.	100.	2.7581	2.9250	2.9199
96.	200.	2.9670	2.9776	2.9504

Table 2

TOTAL Z WIDTH (WITHOUT QCD)

MZ	MT	MH=10	MH=100	MH=1000 GEV
90.	50.	2.2924	2.2948	2.2870
90.	100.	2.3011	2.3035	2.2958
90.	150.	2.3112	2.3137	2.3062
90.	200.	2.3249	2.3275	2.3203
90.	230.	2.3349	2.3376	2.3305
91.	50.	2.3872	2.3898	2.3818
91.	100.	2.3966	2.3993	2.3913
91.	150.	2.4072	2.4099	2.4022
91.	200.	2.4215	2.4244	2.4169
91.	230.	2.4319	2.4349	2.4276
92.	50.	2.4847	2.4876	2.4793
92.	100.	2.4949	2.4978	2.4897
92.	150.	2.5059	2.5090	2.5010
92.	200.	2.5208	2.5240	2.5163
92.	230.	2.5316	2.5349	2.5274
93.	50.	2.5848	2.5880	2.5795
93.	100.	2.5959	2.5992	2.5908
93.	150.	2.6074	2.6108	2.6026
93.	200.	2.6229	2.6264	2.6185
93.	230.	2.6341	2.6377	2.6301
94.	50.	2.6875	2.6911	2.6823
94.	100.	2.6997	2.7033	2.6946
94.	150.	2.7117	2.7154	2.7070
94.	200.	2.7277	2.7316	2.7235
94.	230.	2.7393	2.7433	2.7355
95.	50.	2.7928	2.7968	2.7878
95.	100.	2.8062	2.8102	2.8013
95.	150.	2.8187	2.8228	2.8141
95.	200.	2.8353	2.8396	2.8313
95.	230.	2.8473	2.8517	2.8437
96.	50.	2.9005	2.9049	2.8956
96.	100.	2.9155	2.9199	2.9107
96.	150.	2.9284	2.9330	2.9241
96.	200.	2.9457	2.9504	2.9418
96.	230.	2.9580	2.9629	2.9547

HADRONIC DECAY WIDTHS

Table 3b

		D QUARKS			B QUARKS			U QUARKS		
MZ	MT	MH=10	100	1000	10	100	1000	MH=10	100	1000
90.	50.	0.3478	0.3481	0.3468	0.3440	0.3443	0.3430	0.2681	0.2682	0.2670
90.	100.	0.3495	0.3497	0.3484	0.3445	0.3448	0.3435	0.2695	0.2696	0.2684
90.	150.	0.3516	0.3519	0.3506	0.3439	0.3442	0.3430	0.2713	0.2714	0.2703
90.	200.	0.3546	0.3549	0.3536	0.3430	0.3433	0.3422	0.2738	0.2739	0.2728
90.	230.	0.3568	0.3571	0.3558	0.3423	0.3426	0.3415	0.2756	0.2757	0.2746
91.	50.	0.3629	0.3632	0.3619	0.3590	0.3593	0.3580	0.2807	0.2808	0.2796
91.	100.	0.3646	0.3649	0.3636	0.3595	0.3599	0.3586	0.2822	0.2823	0.2811
91.	150.	0.3668	0.3671	0.3658	0.3589	0.3593	0.3580	0.2841	0.2842	0.2830
91.	200.	0.3699	0.3702	0.3689	0.3579	0.3583	0.3571	0.2867	0.2868	0.2857
91.	230.	0.3721	0.3725	0.3712	0.3571	0.3575	0.3564	0.2886	0.2887	0.2876
92.	50.	0.3782	0.3786	0.3772	0.3742	0.3746	0.3733	0.2937	0.2938	0.2925
92.	100.	0.3800	0.3804	0.3791	0.3749	0.3753	0.3740	0.2953	0.2954	0.2942
92.	150.	0.3823	0.3827	0.3814	0.3743	0.3747	0.3734	0.2973	0.2974	0.2962
92.	200.	0.3855	0.3859	0.3846	0.3732	0.3736	0.3724	0.3000	0.3002	0.2990
92.	230.	0.3878	0.3882	0.3869	0.3723	0.3728	0.3717	0.3020	0.3021	0.3010
93.	50.	0.3939	0.3943	0.3929	0.3898	0.3903	0.3889	0.3070	0.3072	0.3059
93.	100.	0.3958	0.3962	0.3949	0.3906	0.3911	0.3897	0.3088	0.3089	0.3077
93.	150.	0.3981	0.3986	0.3973	0.3899	0.3904	0.3891	0.3109	0.3110	0.3098
93.	200.	0.4014	0.4019	0.4005	0.3888	0.3893	0.3881	0.3137	0.3139	0.3126
93.	230.	0.4038	0.4043	0.4030	0.3878	0.3883	0.3872	0.3157	0.3160	0.3147
94.	50.	0.4098	0.4103	0.4089	0.4057	0.4062	0.4048	0.3208	0.3210	0.3196
94.	100.	0.4119	0.4124	0.4110	0.4067	0.4072	0.4058	0.3227	0.3229	0.3215
94.	150.	0.4143	0.4149	0.4135	0.4060	0.4065	0.4052	0.3248	0.3251	0.3238
94.	200.	0.4177	0.4182	0.4169	0.4047	0.4053	0.4041	0.3278	0.3280	0.3268
94.	230.	0.4202	0.4207	0.4194	0.4036	0.4042	0.4031	0.3299	0.3302	0.3289
95.	50.	0.4261	0.4267	0.4253	0.4219	0.4225	0.4211	0.3349	0.3352	0.3338
95.	100.	0.4284	0.4290	0.4275	0.4231	0.4237	0.4223	0.3370	0.3372	0.3358
95.	150.	0.4309	0.4315	0.4301	0.4223	0.4229	0.4216	0.3392	0.3395	0.3381
95.	200.	0.4343	0.4349	0.4336	0.4210	0.4216	0.4204	0.3423	0.3426	0.3413
95.	230.	0.4369	0.4375	0.4362	0.4198	0.4205	0.4194	0.3445	0.3448	0.3435
96.	50.	0.4427	0.4434	0.4419	0.4384	0.4390	0.4376	0.3494	0.3497	0.3483
96.	100.	0.4452	0.4458	0.4444	0.4398	0.4405	0.4391	0.3517	0.3520	0.3505
96.	150.	0.4478	0.4484	0.4470	0.4390	0.4397	0.4384	0.3540	0.3543	0.3529
96.	200.	0.4513	0.4520	0.4506	0.4376	0.4383	0.4371	0.3572	0.3575	0.3562
96.	230.	0.4540	0.4547	0.4533	0.4363	0.4371	0.4360	0.3595	0.3599	0.3585

Table 3a

LEPTONIC DECAY WIDTHS

		NEUTRINO			ELECTRON		
MZ	MT	MH=10	100	1000	10	100	1000
90.	50.	0.1592	0.1595	0.1592	0.0795	0.0796	0.0794
90.	100.	0.1597	0.1600	0.1597	0.0797	0.0799	0.0797
90.	150.	0.1603	0.1606	0.1603	0.0800	0.0802	0.0800
90.	200.	0.1612	0.1615	0.1612	0.0804	0.0805	0.0804
90.	230.	0.1618	0.1622	0.1619	0.0806	0.0808	0.0807
91.	50.	0.1645	0.1649	0.1645	0.0823	0.0825	0.0823
91.	100.	0.1650	0.1654	0.1651	0.0826	0.0828	0.0826
91.	150.	0.1657	0.1660	0.1657	0.0830	0.0831	0.0829
91.	200.	0.1666	0.1669	0.1666	0.0834	0.0835	0.0834
91.	230.	0.1672	0.1676	0.1673	0.0837	0.0838	0.0837
92.	50.	0.1700	0.1703	0.1700	0.0854	0.0856	0.0853
92.	100.	0.1705	0.1709	0.1706	0.0858	0.0859	0.0857
92.	150.	0.1712	0.1716	0.1712	0.0861	0.0863	0.0861
92.	200.	0.1721	0.1725	0.1722	0.0866	0.0868	0.0866
92.	230.	0.1728	0.1732	0.1729	0.0869	0.0871	0.0869
93.	50.	0.1755	0.1759	0.1756	0.0887	0.0888	0.0885
93.	100.	0.1761	0.1765	0.1762	0.0891	0.0892	0.0889
93.	150.	0.1768	0.1772	0.1769	0.0895	0.0896	0.0894
93.	200.	0.1778	0.1782	0.1779	0.0900	0.0902	0.0900
93.	230.	0.1785	0.1789	0.1786	0.0904	0.0905	0.0903
94.	50.	0.1812	0.1816	0.1813	0.0921	0.0923	0.0920
94.	100.	0.1818	0.1823	0.1819	0.0926	0.0927	0.0924
94.	150.	0.1825	0.1830	0.1827	0.0930	0.0932	0.0929
94.	200.	0.1835	0.1840	0.1837	0.0936	0.0938	0.0935
94.	230.	0.1843	0.1847	0.1844	0.0940	0.0941	0.0939
95.	50.	0.1870	0.1874	0.1871	0.0958	0.0959	0.0956
95.	100.	0.1877	0.1881	0.1878	0.0963	0.0964	0.0961
95.	150.	0.1884	0.1889	0.1885	0.0967	0.0969	0.0966
95.	200.	0.1894	0.1899	0.1896	0.0974	0.0975	0.0973
95.	230.	0.1902	0.1907	0.1903	0.0978	0.0980	0.0977
96.	50.	0.1928	0.1933	0.1930	0.0995	0.0997	0.0993
96.	100.	0.1936	0.1941	0.1938	0.1001	0.1002	0.0999
96.	150.	0.1944	0.1949	0.1946	0.1006	0.1008	0.1005
96.	200.	0.1954	0.1959	0.1956	0.1013	0.1015	0.1012
96.	230.	0.1962	0.1967	0.1964	0.1018	0.1019	0.1017

Table 4

m_t	$\bar{\Gamma}^0_Z(d\bar{d})$	$\Delta\Gamma^{weak}_Z(d\bar{d})$	$\bar{\Gamma}^0_Z(b\bar{b})$	$\Delta\Gamma^{weak}_Z(b\bar{b})$
50	0.3784	0.0001	0.3748	-0.0002
100	0.3809	-0.0005	0.3773	-0.0020
150	0.3838	-0.0011	0.3801	-0.0055
200	0.3875	-0.0017	0.3839	-0.0102
230	0.3904	-0.0021	0.3867	-0.0139

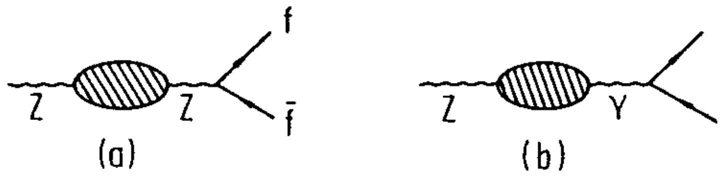

Fig. 1

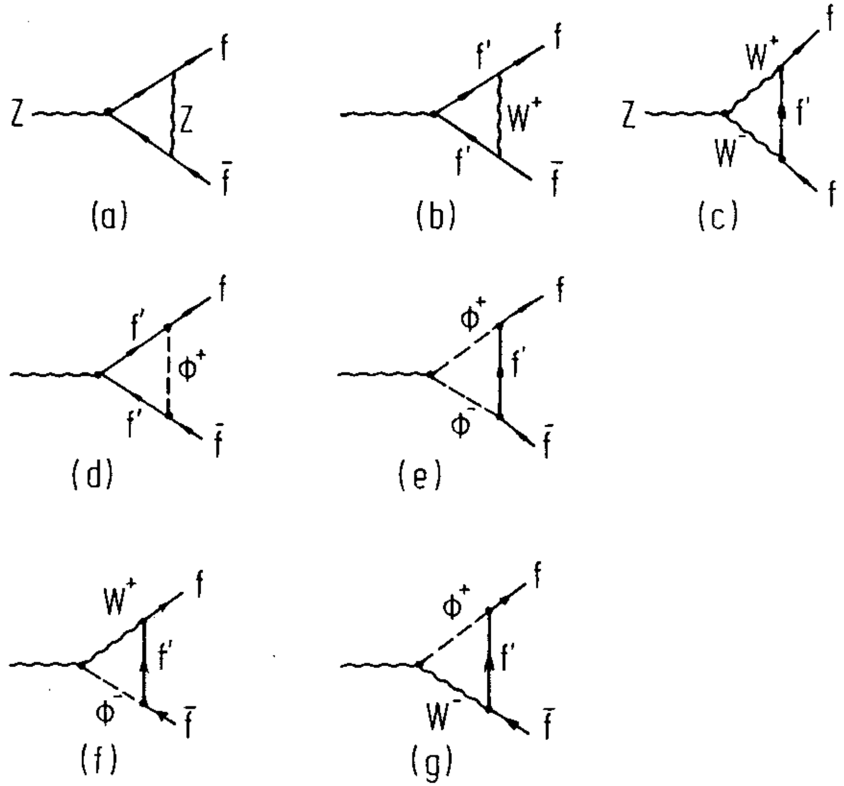

Fig. 2

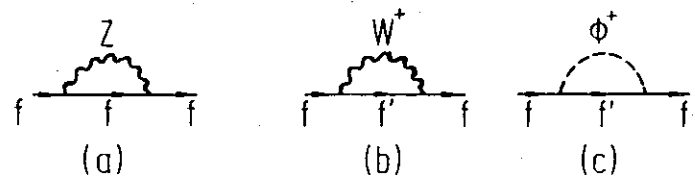

Fig. 3